Saarakkala, Seppo; Alahäivälä, Antti; Hinkkanen, Marko; Luomi, Jorma

Dynamic emulation of multi-mass mechanical loads in electric drives

Published in:
14th European Conference on Power Electronics and Applications (EPE 2011)

Published: 30/08/2011

Document Version
Peer reviewed version

Please cite the original version:
Saarakkala, S., Alahäivälä, A., Hinkkanen, M., & Luomi, J. (2011). Dynamic emulation of multi-mass mechanical loads in electric drives. In *14th European Conference on Power Electronics and Applications (EPE 2011)*

Dynamic emulation of multi-mass mechanical loads in electric drives

Seppo Saarakkala, Antti Alahäivälä, Marko Hinkkanen and Jorma Luomi
AALTO UNIVERSITY
School of Electrical Engineering
P.O. Box 13000
FI-00076 Aalto, Helsinki, Finland
E-mails: seppo.saarakkala@aalto.fi, antti.alahaivala@aalto.fi,
marko.hinkkanen@aalto.fi, jorma.luomi@aalto.fi

Acknowledgments

The authors gratefully acknowledge ABB Oy for the financial support.

Keywords

≪Dynamic emulation≫, ≪Electric drive≫, ≪Elevator≫, ≪Multi-mass system≫

Abstract

This paper presents a straightforward method for dynamic emulation of multi-mass systems. The test bench consists of a driving motor coupled rigidly to a load servo motor, and the torque reference of the servo motor is controlled based on the dynamic model to be emulated. No additional measurements are needed, but the mechanical parameters of the test bench and the torque estimate of the driving motor have to be known. The use of the torque estimate makes it possible to avoid using any differentiations or controller compensation terms in the emulator. The experimental results show that the emulator can model the dynamics of the multi-mass mechanical load with a good accuracy. In addition, the robustness against the mechanical parameter inaccuracies is good.

Introduction

In many applications, the dynamics of an electric drive depend on a complex mechanical system that can be modeled as a multi-mass system. Experiments with such systems can be replaced with dynamic emulation if the driving motor is connected to a controlled load machine. The torque of the load machine is used for mimicking the dynamic behavior of the complex mechanics.

The emulation of mechanical loads for electric drives has been studied in several papers. Emulation has conventionally been used to produce a static load for steady-state tests as in [1] and [2]. A basic strategy for dynamic emulation is the principle of inverse mechanical dynamics (IMD), which is briefly discussed in [3] and [4]. According to the IMD principle, the shaft speed or position of the driving motor is measured and used for calculating the load torque for the load machine. Emulation models and results based on the IMD principle are also presented in [2] and [5]. However, the IMD principle has some drawbacks. It may lead to unstable and noisy results when it is used in a discrete closed-loop control system [3]. Noise in the output is caused by derivative terms in the inverse transfer function. In addition, an inverse model cannot be composed for nonlinear loads.

A common method to avoid the drawbacks of the IMD is to compensate speed or position control loop dynamics and add the feedforward of inverse emulated dynamics from the speed (or position) to the torque [3], [6] and [7]. Adding the feedforward removes the load dynamics from a compensation term, which improves the emulation. This method preserves the dynamics of the emulated load in both open- and closed-loop systems. In [4], the same method is studied using a position control loop. Furthermore, it provides satisfying results in nonlinear systems as seen in [3], [4] and [6]. The method may become complex if an advanced nonlinear controller is needed because the controller is included in the compen-

sation. [8] and [9] present a method to avoid this problem by simply removing the control dynamics from the compensator. These papers also show successful emulation of nonlinear loads.

As mentioned before, emulation provides a practical solution for investigating different drive applications. One interesting application is an elevator, which is studied in this paper. A conventional method for elevator control testing requires an elevator test tower, which asks for great investments and a large amount of space. In addition, testing under different loading conditions may require a use of heavy physical masses. An elevator test tower is used for example in [10] and [11]. Publications on the emulation of elevator systems are rare in the literature, but one implementation is presented in [12]. The paper models an elevator system as a single-mass system and a three-mass system, from which the load torque reference emulating the system is solved and fed to a load machine. However, the accuracy of the method is not discussed in detail. Thus, a demand for a further study exists.

This paper presents a straightforward and practical method for dynamic emulation of multi-mass systems. The test bench consists of a driving motor coupled rigidly to a load servo motor, and the torque reference of the servo motor is controlled based on the dynamic model to be emulated. The angular speed and position are measured, and the electromagnetic torque of the driving motor has to be estimated. The use of the torque estimate makes it possible to avoid using any inverse transfer functions or controller compensation terms in the emulator, thus reducing noise problems and simplifying the method. The emulator is applied to the dynamics of a nonlinear elevator system.

The contents of the paper are the following. First, mechanical models of the test banch and an elevator system are derived. Secondly, the experimental setup (test bench) is described. Then the emulator is experimentally validated by measuring the frequency response and comparing it with the analytical one. The mechanical parameter inaccuracies of the test bench are also considered. Finally, the elevator emulator is tested in closed-loop position control.

Mechanical system modeling

In this section, first the mechanical model of the physical test bench and the emulated nonlinear dynamics are introduced. By using the mechanical models, the torque reference for the load machine is derived.

Test bench

The experimental system consists of mechanically coupled driving and load machines. The coupling between the machines is assumed to be rigid. The mechanical model of the experimental system can be expressed simply as

$$J\ddot{\theta}_{\mathrm{m}} + b\dot{\theta}_{\mathrm{m}} = T_{\mathrm{e}} - T_{\mathrm{l}} \tag{1}$$

where J is the total moment of inertia of the experimental system, b is the viscous damping, θ_{m} is the angular position of the rotor, T_{e} is the electromagnetic torque of the driving motor and T_{l} is the torque reference of the load machine.

Emulated mechanics

The dynamical model of the emulated elevator system is derived in this section. The elevator is modeled as a three-mass system as shown in Fig. 1. The system model consists of the masses of the cage $m_{1,\mathrm{em}}$ and the counterweight $m_{2,\mathrm{em}}$, and the inertia of the sheave J_{em}. The ropes are modeled to be elastic [10]. The mechanical dynamics of an elevator can be described by five equations:

$$J_{\mathrm{em}}\ddot{\theta}_{\mathrm{m}} + b_{\mathrm{em}}\dot{\theta}_{\mathrm{m}} = T_{\mathrm{e}} - R_{\mathrm{em}}F_{\mathrm{s1,em}} - R_{\mathrm{em}}F_{\mathrm{s2,em}} \tag{2}$$

$$F_{\mathrm{s1,em}} = k_{1,\mathrm{em}}(R_{\mathrm{em}}\theta_{\mathrm{m}} - x_{\mathrm{l,em}}) + c_{1,\mathrm{em}}(R_{\mathrm{em}}\dot{\theta}_{\mathrm{m}} - \dot{x}_{\mathrm{l,em}}) \tag{3}$$

$$F_{\mathrm{s2,em}} = k_{2,\mathrm{em}}(R_{\mathrm{em}}\theta_{\mathrm{m}} - x_{2,\mathrm{em}}) + c_{2,\mathrm{em}}(R_{\mathrm{em}}\dot{\theta}_{\mathrm{m}} - \dot{x}_{2,\mathrm{em}}) \tag{4}$$

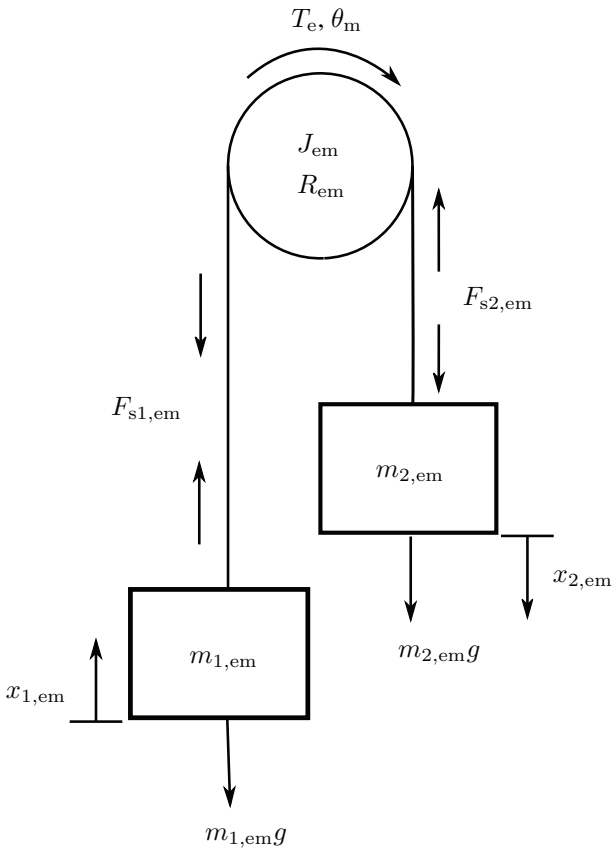

Fig. 1: The emulated elevator system.

$$m_{1,\mathrm{em}}\ddot{x}_{1,\mathrm{em}} = F_{\mathrm{s}1,\mathrm{em}} - m_{1,\mathrm{em}}g \tag{5}$$

$$m_{2,\mathrm{em}}\ddot{x}_{2,\mathrm{em}} = F_{\mathrm{s}2,\mathrm{em}} + m_{2,\mathrm{em}}g \tag{6}$$

where $F_{\mathrm{s}1,\mathrm{em}}$ and $F_{\mathrm{s}2,\mathrm{em}}$ are the forces acting on the elevator ropes, and R_em is the radius of the sheave. The spring constants $k_{1,\mathrm{em}}$, $k_{2,\mathrm{em}}$ and the damping constants $c_{1,\mathrm{em}}$, $c_{2,\mathrm{em}}$ of both-side ropes depend linearly on the displacement of the cage $x_{1,\mathrm{em}}$ or the counterweight $x_{2,\mathrm{em}}$. The dependencies are given by

$$k_{1,\mathrm{em}} = k_{\mathrm{x,em}}x_{1,\mathrm{em}} + k_{01,\mathrm{em}} \tag{7}$$

$$k_{2,\mathrm{em}} = -k_{\mathrm{x,em}}x_{2,\mathrm{em}} + k_{02,\mathrm{em}} \tag{8}$$

$$c_{1,\mathrm{em}} = c_{\mathrm{x,em}}x_{1,\mathrm{em}} + c_{01,\mathrm{em}} \tag{9}$$

$$c_{2,\mathrm{em}} = -c_{\mathrm{x,em}}x_{2,\mathrm{em}} + c_{02,\mathrm{em}} \tag{10}$$

where $k_{\mathrm{x,em}}$, $k_{01,\mathrm{em}}$ and $k_{02,\mathrm{em}}$ are spring constant parameters, and $c_{\mathrm{x,em}}$, $c_{01,\mathrm{em}}$ and $c_{02,\mathrm{em}}$ are damping constant parameters.

The torque reference of the load machine can be derived from (1) and (2)−(6). The result is

$$T_\mathrm{l} = \left(1 - \frac{J}{J_\mathrm{em}}\right) T_\mathrm{e} + \frac{J}{J_\mathrm{em}} R_\mathrm{em}(F_{\mathrm{s}1,\mathrm{em}} + F_{\mathrm{s}2,\mathrm{em}}) + \left(\frac{J}{J_\mathrm{em}} b_\mathrm{em} - b\right) \dot{\theta}_\mathrm{m} \tag{11}$$

The effective height of the emulated elevator system is 50 meters. The system parameters were downscaled to meet limitations of the test bench. The downscaled constant parameters of the emulated elevator system are presented in Table I.

Table I: The parameters used in the elevator system emulation.

Parameter	Value
Sheave inertia J_{em} (kgm^2)	0.044
Viscous damping b_{em} (Nms)	0.02
Counterweight mass $m_{2,\mathrm{em}}$ (kg)	9.6
Mass of the empty elevator cage $m_{1,\mathrm{em},0}$ (kg)	6.4
Radius of the sheeve R_{em} (m)	0.25
Rope spring parameter $k_{\mathrm{x,em}}$ (N/m^2)	-39.76
Rope damping parameter $c_{\mathrm{x,em}}$ (Ns/m^2)	-0.1485
Total inertia of the experimental system (nominal) J (kgm^2)	0.02
Viscous damping of the experimental system (nominal) b (Nms)	0.02

Table II: Case dependent elevator model parameters.

Parameter	Case 1	Case 2
$k_{01,\mathrm{em}}$ (N/m)	2012	3006
$k_{02,\mathrm{em}}$ (N/m)	4000	3006
$c_{01,\mathrm{em}}$ (Ns/m)	3.4	7.1
$c_{02,\mathrm{em}}$ (Ns/m)	10.8	7.1
$m_{1,\mathrm{em}}$ (kg)	12.8	9.6
$x_{1,\mathrm{em}}$ (m) $\in$	[0,50]	[$-$25,25]
$x_{2,\mathrm{em}}$ (m) $\in$	[0,50]	[$-$25,25]
θ_{m} (rad) $\in$	[0,200]	[$-$100,100]

It is to be noted that in (7)$-$(10) the slopes of the linear dependencies will be the same all the time, but the initial parts and the coordinate system depend on the selected initial positions of the elevator cage and the counterweight. Two cases are studied in the following. In Case 1, the initial position of the elevator cage is downstairs and the elevator cage is full ($m_{1,\mathrm{em}} = 12.8$ kg). In Case 2, the initial position of the elevator cage is in the middle of the operating region and the elevator cage is half full ($m_{1,\mathrm{em}} = 9.6$ kg). The case dependent parameters are presented in Table II.

Experimental setup

The test system consists of two mechanically coupled permanent magnet synchronous machines (PMSMs) and two frequency converters, which are controlled by a dSPACE DS1103 PPC digital controller. The basic structure of the experimental setup is presented in Fig. 2. The driving motor is a 2.2-kW six-pole PMSM. It is fed by a frequency converter and the control of the motor is based on rotor-oriented vector control. The rated torque of the driving motor is 14 Nm. The bandwidth of the current control for the tested machine is selected to be 225 Hz, which is significantly higher than the highest resonance frequency to be emulated. A pulse encoder is used as a feedback from the driving machine to produce the angular position information that is sampled with 2048 pulses per revolution. The angular speed is calculated from the measured angular position difference within the fixed sampling interval of 200 μs. The desribed method causes quantification noise especially at low rotational speeds, and it is of interest to see how sensitive the emulation method is to the quantification noise.[1] The load consist of a PMSM servo drive that uses an ABB BIVECTOR 535 ”25” frequency converter. The rated speed and the continous stall torque of the load motor are 3000 rpm and 21.5 Nm, respectively. The load motor is torque-controlled, and the reference is calculated in the DS1103 from where it is fed to the converter as an analog signal.

[1] By using more advanced signal processing algorithms, the noise level of the measured angular speed could be reduced.

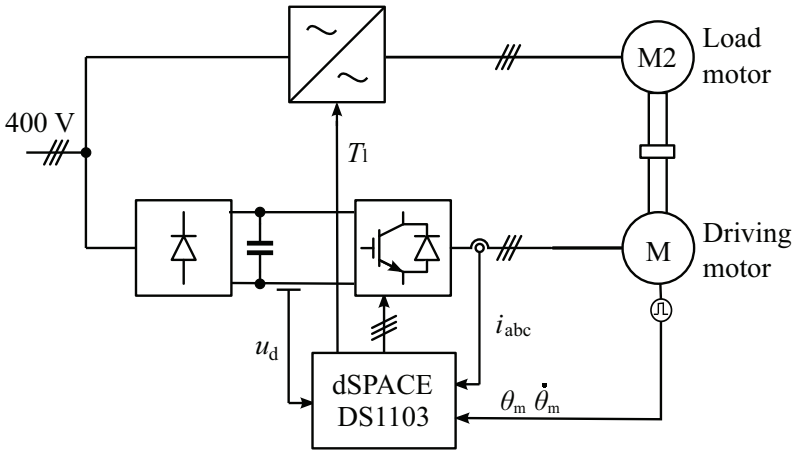

Fig. 2: Experimental setup. i_abc and u_d are the motor currents and the DC-link voltage, respectively. T_l is the load torque reference for the load machine.

Model validation

In this section, the nonlinear emulation model, consisting of (2)−(11), is validated by measuring its frequency response and comparing the result with the analytical frequency response. The frequency responses are measured from the electromagnetic torque of the driving motor to the angular speed of the motor.

Because the frequency response technique is applicable only for linear systems, the analytical frequency response is formed for the linearized system. For the experimental frequency response, a sine wave is fed into the control system as a torque reference $T_\mathrm{e,ref}$. The frequency of the sine wave varies from 1.6 Hz to 17.5 Hz with a resolution of 0.08 Hz. Each frequency is fed for 20 periods and the data, T_e and $\dot{\theta}_\mathrm{m}$, are recorded when the system is fully woken. These signals are transformed into the frequency domain by the discrete Fourier transformation (DFT) [13] in order to find the gain and the phase shift of the signals. The amplitude of the reference sine wave is 3 Nm at every frequency. For the experimental frequency response, the gravitation is also neglected to avoid the need of controller for the compensation of mass imbalance.

In order to study the emulator robustness against the experimental system parameter (J and b) uncertainties, the frequency response is measured for the cases where one of the parameters is 15% over estimated or under estimated, while at the same time the other one is kept at its nominal value.

In Case 1, the parameters are selected to produce two resonances and two anti-resonances. As can be seen in Fig. 3(a), the emulator generates the dynamic bahavior of the elevator successfully. It is worth noticing that the resonance frequencies are lowered if the total inertia of the test system is estimated to be too low. On the other hand, the resonances are at too high frequencies if the total inertia of the test system is estimated to be too high. However, the errors in the dynamic behavior are not significant. It can be concluded that the emulator robustness against the total inertia uncertainty is good. An incorrect value for the estimate of the viscous damping b has a minor effect on the emulation accuracy. These results are not shown here.

In Case 2, the cage and the counterweight have the same antiresonance frequency. Therefore, only one resonance and anti-resonance occur as seen in Fig. 3(b). The emulator again provides a successful frequency response. The robustness against the parameter uncertainties is similar to Case 1.

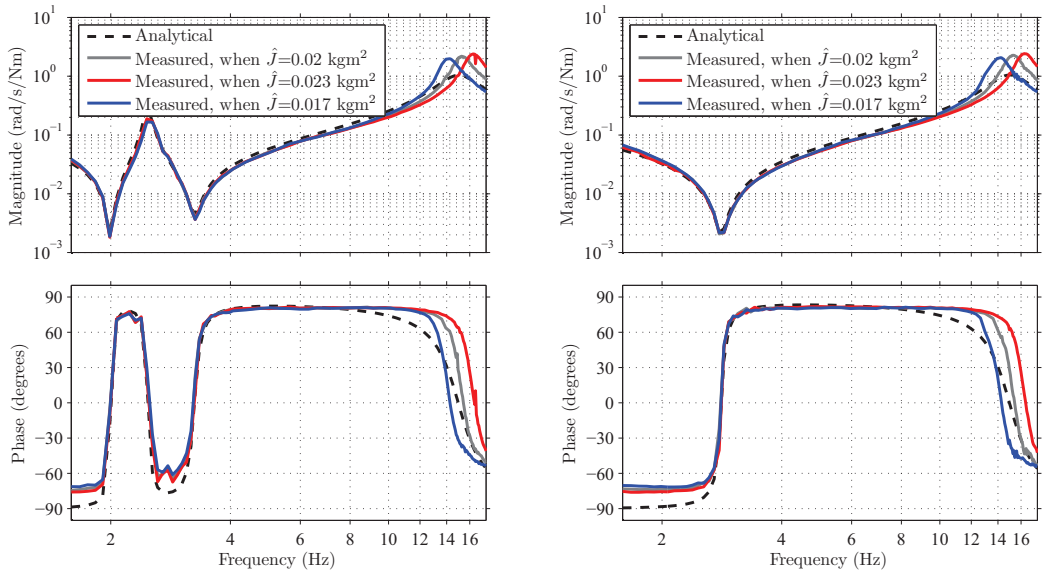

(a) (b)

Fig. 3: The measured (solid lines) and the analytical (dashed line) frequency responses from electromagnetic torque of the driving motor to the angular speed of the motor: (a) Case 1, (b) Case 2

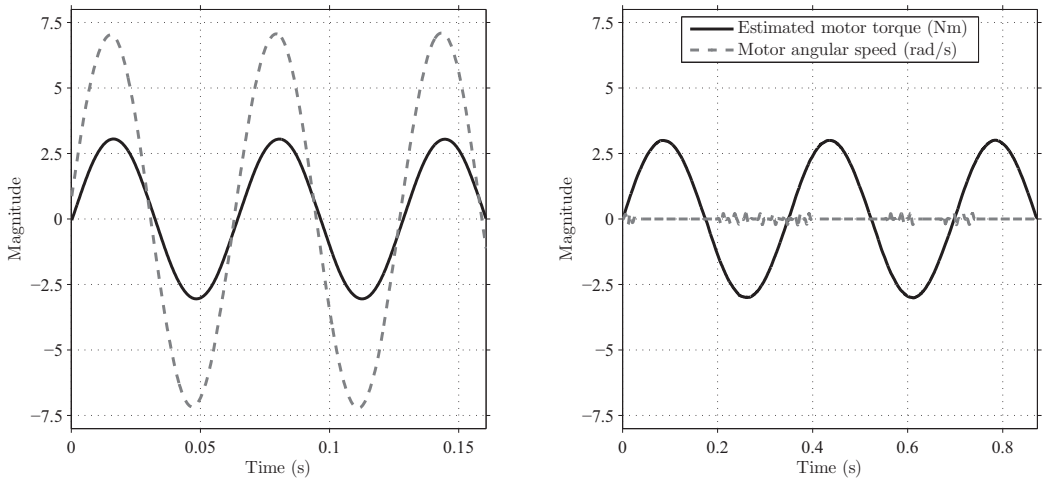

(a) (b)

Fig. 4: Estimated motor torque (solid line) and measured motor speed (dashed line): (a) resonance frequency is fed to the system, (b) antiresonance frequency is fed to the system.

Fig. 4(a) shows the response of the emulator system when a sine wave at the resonance frequency is used as a torque reference, and Fig. 4(b) shows the response of the emulator system when a sine wave at the antiresonance frequency is used as a torque reference. It can be clearly seen that at the resonance frequency, the system has a high gain and no phase shift. At the antiresonance frequency, the system has almost zero gain.

Operation under position control

In this section, the operation of the emulator is studied when the emulated elevator system is position controlled. First, a simple rigid body control is designed, and then the elevator system is driven from upstairs to downstairs with two different elevator cage masses.

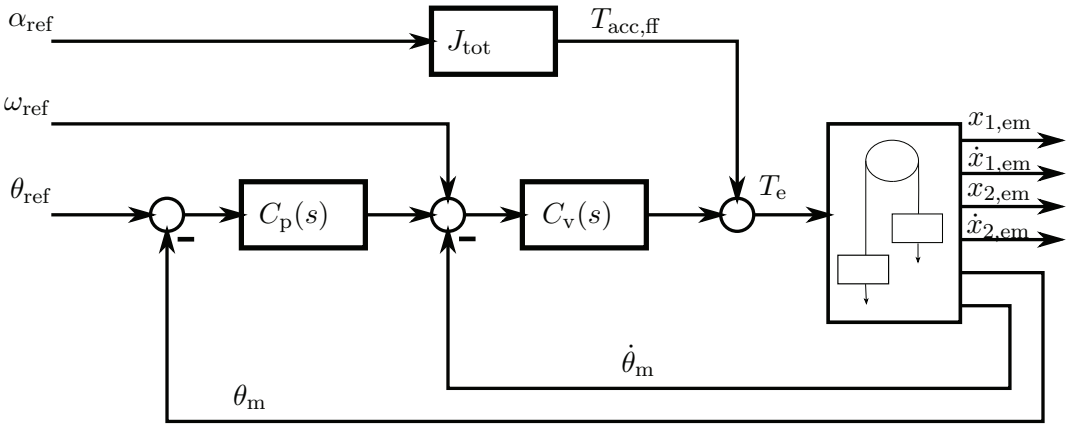

Fig. 5: Position controlled elevator system. ω_{ref} and α_{ref} are the motor angular velocity and acceleration references, respectively

Control design

A cascaded position control structure is designed for the elevator system. The control structure is shown in Fig. 5.

The speed control loop is first closed. Because the main focus in this work is not in the field of control design, a simple internal model PI-controller design technique (IMC) for rigid body systems is used here [14]. The transfer function of the PI controller $C_{\mathrm{v}}(s)$ is given as

$$C_{\mathrm{v}}(s) = k_{\mathrm{p}} + \frac{k_{\mathrm{i}}}{s} \tag{12}$$

In the IMC design, the total inertia J_{tot} of the system, the viscous damping b_{em} of the system and the chosen bandwidth α_{s} of the closed speed control loop are the design parameters. The total inertia can be estimated to be at least $J_{\mathrm{tot}} = J_{\mathrm{em}} + (m_{1,\mathrm{em},0} + m_{2,\mathrm{em}})R_{\mathrm{em}}^2 = 1.044$ kgm^2. The motor angular speed and angular position are selected as the feedback signals according to Fig. 5. Because of the antiresonance behavior, which can be seen in the motor-side, it is in a favour of a good control design to set the bandwidth of the closed-loop control system below the lowest antiresonance frequency, which exists in the motor-side (in this case below 2 Hz). For the speed control, the bandwidth of 1 Hz is selected. With these selections, the parameters of the speed controller in (12) can be selected as $k_{\mathrm{p}} = \alpha_{\mathrm{s}} J_{\mathrm{tot}}$ and $k_{\mathrm{i}} = \alpha_{\mathrm{s}} b_{\mathrm{m,em}}$. Because of the noise caused by the quantification of the speed and position measurement, the speed error is filtered using a first-order low-pass filter with the cut-off frequency of 200 Hz.

After the speed controller is designed, the outer position control loop is to be closed. Let us use pure gain as a position controller: $C_{\mathrm{p}}(s) = k_{\mathrm{pp}}$. If the gain $k_{\mathrm{pp}} = \alpha_{\mathrm{s}}/4$ is selected, the closed position control loop will have a bandwidth of $\alpha_{\mathrm{s}}/3$ and it will be critically damped. Furthermore in order to get better reference tracking capability, a simple acceleration feedforward $T_{\mathrm{acc,ff}} = J_{\mathrm{tot}}\alpha_{\mathrm{ref}}$ is used.

Measurements

The operation of the emulated elevator system is tested during typical elevator motion. In Case 1, the elevator cage is initially downstairs, and it is driven upstairs to see the operation during the upward motion. In Case 2, the elevator is initially in the middle of the operating area, and it is first driven up. After a short recovery time it is driven downstairs to also see the operation during the downward motion. The desired position trajectories of the elevator cage for Case 1 and Case 2 are shown in Figs. 6(a) and 6(b), respectively. To produce the reference trajectories shown in Fig. 6, the references for the position control system are selected according to Table III.

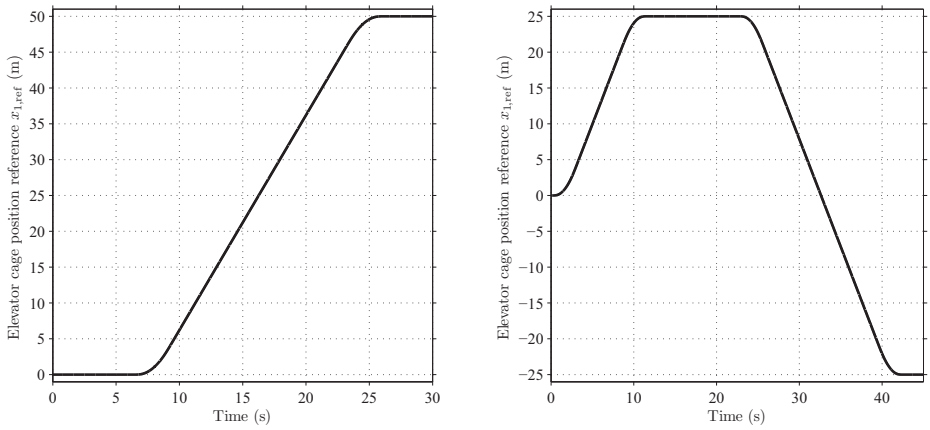

(a) (b)

Fig. 6: Elevator cage position trajectories for the motion control tests: (a) Case 1, (b) Case 2.

Table III: Motor reference trajectory values for motion tests.

Parameter	Case 1	Case 2
Motor angular position θ_{ref} (rad)	$0 \rightarrow 200$	$0 \rightarrow 100 \rightarrow$ -100
Motor angular velocity ω_{ref} (rad/s)	12	12
Motor angular acceleration and deceleration α_{ref} (rad/s^2)	5	5
Motor angular jerk $\dot{\alpha}_{\mathrm{ref}}$ (rad/s^3)	8	8

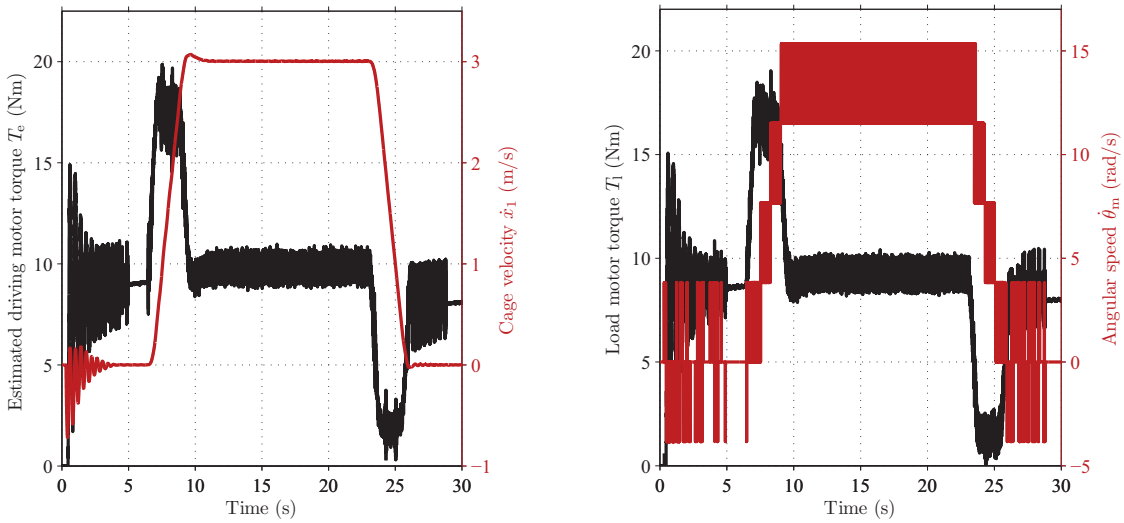

(a) (b)

Fig. 7: Measurement results for Case 1: (a) estimated electromagnetic torque of the driving motor (black line) and emulated elevator cage velocity (gray line), (b) torque reference of the load machine (black line) and measured angular velocity of the driving motor (gray line).

In Fig. 7(a), the estimate of the electromagnetic torque of the driving motor and the emulated velocity of the elevator cage are shown for Case 1. In Fig. 7(b), the torque reference for the load machine and the measured speed of the driving motor are shown for Case 1.

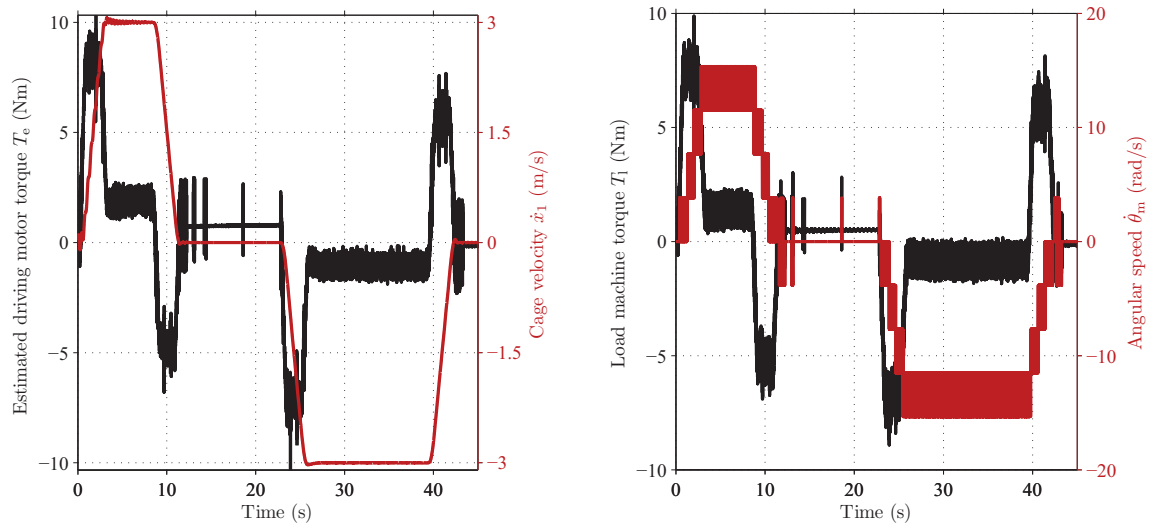

(a) (b)

Fig. 8: Measurement results for Case 2: (a) estimated electromagnetic torque of the driving motor (black line) and emulated elevator cage velocity (gray line), (b) torque reference of the load machine (black line) and measured angular velocity of the driving motor (gray line).

It can be seen in Fig. 7 that an offset torque occurs. It is caused by the mass imbalance between the elevator cage and the counterweight. It should be noted that low-frequency oscillations occur during the first 7 seconds, because of the existence of the lower resonance frequency at the initial position of Case 1.

In Fig. 8(a) the estimate of the electromagnetic torque of the driving motor and the emulated velocity of the elevator cage are shown for Case 2. In Fig. 8(b) the torque reference for the load machine and the measured speed of the driving motor are shown for Case 2.

It can be seen in Fig. 8 that now there is no offset torque since the elevator cage mass is equivalent to the counterweight mass. No low-frequency oscillations occur initially, because only the higher resonance frequency exists at the initial position of Case 2.

It is worth noticing that despite the high noise level in the estimated electromagnetic torque and particularly in the measured angular speed (because of the encoder quantification noise), the noise level of the load machine torque reference is still acceptable. Based on the measurements, it seems that the noise sensitivity of the emulator is good.

Conclusions

A straightforward method for the dynamic emulation of multi-mass systems was presented in this paper. The emulation method is capable of correctly generating the dynamics of the modeled nonlinear system. The validation also shows that the emulator has a good robustness against the physical parameter uncertainties. Operation under position control also gives good results and shows that the emulation method is not very sensitive to the quantification noise, caused by the angular position and speed measurements. Thus, the emulator can be used in drive control testing, and no real mechanics of the system to be tested are required. The emulator can be easily modified to mimic different mechanics, and it allows the emulation of different parameters and load conditions. Therefore, the setup offers a versatile instrument for drive testing and control design.

References

[1] A. Williamson and K. Al-Khalidi, "An improved engine-testing dynamometer," in *Fourth International Conference on Electrical Machines and Drives*, London, the United Kingdom, Sept. 1989, pp. 374–378.

[2] E. J. Collins and Y. Huang, "A programmable dynamometer for testing rotating machinery using a three-phase induction machine," *IEEE Transactions on Energy Conversion*, vol. 9, pp. 521–527, Sep. 1994.

[3] Z. Hakan Akpolat, G. Asher, and J. Clare, "Dynamic emulation of mechanical loads using a vector-controlled induction motor-generator set," *IEEE Transactions on Industrial Electronics*, vol. 46, no. 2, pp. 370–379, Apr 1999.

[4] J. Arellano-Padilla, G. Asher, and M. Sumner, "Control of an ac dynamometer for dynamic emulation of mechanical loads with stiff and flexible shafts," *IEEE Transactions on Industrial Electronics*, vol. 53, no. 4, pp. 1250–1260, Jun. 2006.

[5] P. Sandholdt, E. Ritchie, J. Pedersen, and R. Betz, "A dynamometer performing dynamical emulation of loads with nonlinear friction," in *Proceedings of the IEEE International Symposium on Industrial Electronics. ISIE '96*, vol. 2, Warsaw, Poland, Jun. 1996, pp. 873–878.

[6] Z. Hakan Akpolat, G. Asher, and J. Clare, "Experimental dynamometer emulation of non-linear mechanical loads," in *The 1998 IEEE Industry Applications Conference, 1998. Thirty-Third IAS Annual Meeting.*, vol. 1, St. Louis, MO, Oct. 1998, pp. 532–539.

[7] C. Hewson, G. Asher, and M. Sumner, "Dynamometer control for emulation of mechanical loads," in *The 1998 IEEE Industry Applications Conference, 1998. Thirty-Third IAS Annual Meeting.*, vol. 2, St. Louis, MO, Oct. 1998, pp. 1511–1518.

[8] M. Rodic, K. Jezernik, and M. Trlep, "Dynamic emulation of mechanical loads: an advanced approach," *IEE Proceedings on Electric Power Applications*, vol. 153, no. 2, pp. 159–166, Mar. 2006.

[9] ——, "Use of dynamic emulation of mechanical loads in the testing of electrical vehicle driveline control algorithms," in *European Conference on Power Electronics and Applications, EPE*, Aalborg, Denmark, Sept. 2007, pp. 1–10.

[10] J.-K. Kang and S.-K. Sul, "Vertical-vibration control of elevator using estimated car acceleration feedback compensation," *IEEE Transactions on Industrial Electronics*, vol. 47, no. 1, pp. 91–99, Feb. 2000.

[11] M. Osama and O. Abdul Azim, "Implementation and performance analysis of an elevator electric motor drive system," in *12th International Middle-East Power System Conference, 2008. MEPCON 2008.*, Aswan, Egypt, Mar. 2008, pp. 114–118.

[12] H.-M. Ryu, S.-J. Kim, S.-K. Sul, T.-S. Kwon, K.-S. Kim, Y.-S. Shim, and K.-R. Seok, "Dynamic load simulator for high-speed elevator system," in *Proceedings of the Power Conversion Conference. PCC Osaka 2002*, vol. 2, Osaka, Japan, Apr. 2002, pp. 885–889.

[13] J. G. Proakis and D. G. Manolakis, *Introduction to Digital Signal Processing*. New York: Macmillan Publishing Company, 1989.

[14] L. Harnefors, K. Pietiläinen, and L. Gertmar, "Torque-maximizing field-weakening control: Design, analysis, and parameter selection," *IEEE Transactions on Industrial Electronics*, vol. 48, no. 1, pp. 161–168, Feb. 2001.